

# Impact of the molecular resonances on the $^{12}\text{C} + ^{12}\text{C}$ fusion reaction rate

Yasutaka Taniguchi<sup>a,b</sup>, Masaaki Kimura<sup>b</sup>

<sup>a</sup>Department of Information Engineering, National Institute of Technology (KOSEN), Kagawa College, 551 Kohda, Takuma-cho, Mitoyo, 769-1192, Kagawa, Japan

<sup>b</sup>RIKEN Nishina Center, 2-1 Hirosawa, Wako, 351-0198, Saitama, Japan

## Abstract

The properties of the low-energy  $^{12}\text{C} + ^{12}\text{C}$  molecular resonances, which potentially enhance the fusion reaction rate at low temperatures, have been investigated by a full-microscopic nuclear model employing various nuclear energy density functionals. We show that some density functionals plausibly describe the observed high-spin  $^{12}\text{C} + ^{12}\text{C}$  molecular resonances and predict many  $0^+$  and  $2^+$  resonances at low energies, which enhance the reaction rate. We also discuss how the uncertainty in the nuclear energy density functionals propagates to that of the reaction rate.

**Keywords:**  $^{12}\text{C} + ^{12}\text{C}$  fusion reaction rate, X-ray superburst, Microscopic nuclear model

## 1. Introduction

The  $^{12}\text{C} + ^{12}\text{C}$  fusion reaction plays a vital role in explosive phenomena in the universe, such as X-ray superbursts (XRSBs) [1, 2], type Ia supernovae [3, 4], and the evolution of massive stars [5]. Its reaction rate at low temperatures has been of great interest for many years. Recently, direct measurements have reached to the energies as low as  $E \simeq 2$  MeV [6, 7, 8]. In addition, an indirect measurement by the Trojan Horse Method (THM) [9] has reported that resonances below 2 MeV might significantly enhance the reaction rate. However, the reaction rate at low temperatures still remains inconclusive due to the uncertainties in the measurements.

Consequently, the reaction rates extrapolated to low temperatures are used in the simulations of astrophysical phenomena. The standard estimation by Caughlan and Fowler (CF88) [10] assumes a constant modified astrophysical spectroscopic factor ( $S^*$ -factor), whereas the hindrance model [11] asserted its suppression at low temperatures. Contrary, Cooper et al. [12] discussed an increased reaction rate at low temperatures. Thus, there are ad-hoc variations of the reaction rate, and hence, it is crucial to impose a constraint by the nuclear model calculations. In particular, it is an essential task for nuclear theories to investigate whether the resonances increase the reaction rate.

In our previous work [13], on the basis of the antisymmetrized molecular dynamics (AMD) calculations, we discussed the low-energy resonances which affect the  $^{12}\text{C} + ^{12}\text{C}$  fusion reaction. Here, we conduct extensive research, and report the low-energy resonances which have the  $^{12}\text{C} + ^{12}\text{C}$  molecule-like structure and significantly affect the reaction rate. Employing several nuclear density functionals, we assess the constraint on the reaction rate imposed by the nuclear theory.

## 2. Theoretical Model

The description of the low-energy resonances requires an accurate description of various reaction channels and rearrangement of nucleons. To meet this requirement, we employ the generator coordinate method (GCM) [14, 15] which describes a resonance by a superposition of the wave functions for various channels,

$$\Psi^J = \sum_{cIK} f_{cIK} P_{MK}^J \Psi_c(d_i) + \sum_{iK} g_{iK} P_{MK}^J \Psi_{Mg}(\beta_i), \quad (1)$$

where  $P_{MK}^J$  is the angular momentum projector, and  $\Psi_c(d_i)$  is the channel wave function where the subscript  $c$  denotes the channels relevant to the fusion reaction, i.e.,  $^{12}\text{C} + ^{12}\text{C}$ ,  $\alpha + ^{20}\text{Ne}$ , and  $p + ^{23}\text{Na}$  channels. The inter-nuclear distance  $d_i$  ranges from 0.5 to 8 fm for the  $^{12}\text{C} + ^{12}\text{C}$ , from 0.5 to 9 fm for the  $\alpha + ^{20}\text{Ne}$ , and from 0.5 to 7 fm for the  $p + ^{23}\text{Na}$ , with the common intervals of 0.5 fm. In addition, the wave functions of the compound nucleus  $^{24}\text{Mg}$ , denoted by  $\Psi_{Mg}(\beta_i)$ , are also superposed to describe the coupling between the entrance and exit channels and the compound states. The resonance energy and the coefficients  $f_{cIK}$  and  $g_{iK}$  are determined by the diagonalization of the Hamiltonian defined by the density functionals. We have employed several parameter sets of the density functionals, the Gogny parameter sets (D1S [16] and D1M\* [17]) and Skyrme parameter sets (SkM\* [18], SLy4 [19, 20], and SIII [21]).

Each channel wave function is the Slater determinant of the nucleon wave packets projected to positive parity,

$$\Psi = \frac{1 + P_r}{2} \mathcal{A}\{\varphi_1 \cdots \varphi_A\}, \quad (2)$$

where  $P_r$  is the parity operator, and each nucleon is described by Gaussian wave packet [22],

$$\varphi_p = \prod_{\sigma=x,y,z} e^{-\nu_\sigma (r_\sigma - Z_{p\sigma})^2} (a_p |\uparrow\rangle + b_p |\downarrow\rangle) \eta_p, \quad (3)$$

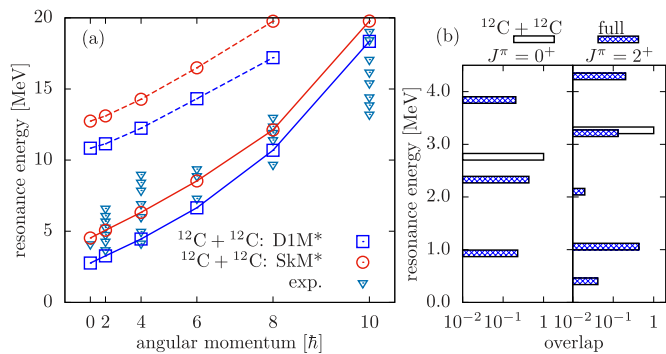


Figure 1: (a) The energies of the  $^{12}\text{C} + ^{12}\text{C}$  molecular resonances calculated by using the DIM\* and SkM\* functionals with only the  $^{12}\text{C} + ^{12}\text{C}$  channel. The lines connect the states with strong E2 transitions. The observed data [25, 26, 27, 28, 29, 30, 31, 32, 33, 34] are also shown for comparison. (b) The energies of the  $^{12}\text{C} + ^{12}\text{C}$  molecular resonances calculated by using the DIM\* functional without (white bars) and with (blue bars) the channel coupling. The lengths of the blue bars indicate the overlap of the wave functions with the  $^{12}\text{C} + ^{12}\text{C}$  channel.

where isospin  $\eta_p$  is fixed to either proton or neutron for all nucleons. The parameter  $\mathbf{Z}_p$  represents the mean position and momentum of each nucleon. By controlling the parameter  $\mathbf{Z}_p$ , the rearrangement of nucleons can be described in a unified manner. In the practical calculations of the  $^{12}\text{C} + ^{12}\text{C}$ ,  $\alpha + ^{20}\text{Ne}$ , and  $p + ^{23}\text{Na}$  channels,  $\mathbf{Z}_p$ , spin ( $a_p$  and  $b_p$ ), and width parameters  $\nu$  are determined by the energy variation with the constraint on the inter-nuclear distance  $d_i$  [23]. Through the variational calculations, the rotation and polarization of nuclei are naturally described depending on the inter-nuclear distance. The wave functions for the compound nucleus  $^{24}\text{Mg}$  are calculated by the energy variation with the constraint on the quadrupole deformation parameter  $\beta$  [24].

### 3. Results and Discussions

Figure 1(a) shows the  $^{12}\text{C} + ^{12}\text{C}$  molecular bands calculated with only the  $^{12}\text{C} + ^{12}\text{C}$  channel, neglecting the coupling with the exit channels and compound states. For comparison, we show the results obtained by using the DIM\* and SkM\* functionals. Both density functionals yield two molecular bands, and the lower one qualitatively reproduces the observed resonances [25, 26, 27, 28, 29, 30, 31, 32, 33, 34] from low to high spin. The DIM\* yields lower resonance energies than the SkM\*, and this trend is common to other parameter sets, i.e., the Gogny functionals always yield lower resonance energies than the Skyrme functionals. This may be due to the finite-range two-body interaction of the Gogny functionals, which gives stronger attraction between two nuclei at large distances. As discussed later, this makes the qualitative difference in the low-temperature reaction rate.

Now, we discuss the channel coupling effects. Figure 1(b) shows how the  $^{12}\text{C} + ^{12}\text{C}$  molecular states are fragmented into many resonances by the channel coupling in the case of the DIM\* functional. The white bars show the energies of the  $J^\pi = 0^+$  and  $2^+$  resonances obtained with only the  $^{12}\text{C} + ^{12}\text{C}$

channel, whereas the blue bars show the resonances obtained by including all channels. The lengths of blue bars indicate the magnitude of the overlap between the wave functions obtained by including all channels and those obtained by including only the  $^{12}\text{C} + ^{12}\text{C}$  channel (white bars). It is clear that the  $^{12}\text{C} + ^{12}\text{C}$  molecular states are fragmented into many resonances due to the channel coupling. Note that some of the resonances are located down to 1 MeV within the Gamow window of the XRSBs. In contrast, Skyrme functionals do not yield the resonances as low as 1 MeV, because the energies of the  $^{12}\text{C} + ^{12}\text{C}$  molecular states without the channel coupling is too high.

We apply the  $R$ -matrix theory [35] and the Breit-Wigner formula [36] to evaluate resonance parameters and  $S^*$ -factors. We calculate the reduced width amplitude (RWA) [37, 38] which is the overlap between the decay channel and resonance wave functions,

$$a^2 y_l^{A_1+A_2}(a) = \sqrt{\binom{24}{A_1}} \langle \delta(r-a) [\Phi_{A_1} \Phi_{A_2} Y_l(\hat{r})]_M' | \Psi_M^{J^\pi} \rangle, \quad (4)$$

where the wave function for the decay channel is composed of nuclei with masses  $A_1$  and  $A_2$  separated by the distance  $a$  with the orbital angular momentum  $l$ . We consider six decay channels,  $\alpha + ^{20}\text{Ne}(0_1^+)$ ,  $\alpha + ^{20}\text{Ne}^*(2_1^+)$ ,  $\alpha + ^{20}\text{Ne}^*(4_1^+)$ ,  $p + ^{23}\text{Na}(3/2_1^+)$ ,  $p + ^{23}\text{Na}^*(5/2_1^+)$ , and  $p + ^{23}\text{Na}^*(7/2_1^+)$ , which are denoted by  $\alpha_0$ ,  $\alpha_1$ ,  $\alpha_2$ ,  $p_0$ ,  $p_1$ , and  $p_2$ , respectively. We also calculated  $\alpha_3$  and  $\alpha_4$  channels and found that they are negligible. The wave functions of  $\alpha$ ,  $^{20}\text{Ne}$ , and  $^{23}\text{Na}$  are also calculated by AMD. In Table 1, we list the RWAs of the resonances as the ratio to the Wigner limit,

$$\theta_{A_1+A_2,l}^2(a) = \frac{a}{3} |a y_l^{A_1+A_2}(a)|^2, \quad (5)$$

where the channel radius  $a$  is chosen to connect the RWAs to the Coulomb wave function smoothly. In principle, if the channel radius  $a$  is sufficiently large so that nuclear force and channel coupling are negligible, the decay width calculated by Eq. (6) does not depend on the choice of channel radius. However, because we performed numerical calculations within a finite spatial size, the decay widths and the reaction rates calculated from them depend on the channel radius. In order to assess this uncertainty, we also made the calculations by artificially changing the channel radius by 1 fm. We found that the reaction rates change by, at most, a factor of two. Thus, the impact of this uncertainty on astrophysical applications is relatively minor, although it cannot be ignored from a nuclear physics perspective. The partial decay width  $\Gamma_{A_1+A_2,l}$  is calculated from the RWA,

$$\Gamma_{A_1+A_2,l} = P_C^{(l)}(a) \frac{3\hbar^2}{2\mu a^2} \theta_{A_1+A_2,l}^2(a). \quad (6)$$

$P_C^{(l)}$  is the Coulomb penetration factor,

$$P_C^{(l)} = \frac{2ka}{F_l^2(ka) + G_l^2(ka)}, \quad (7)$$

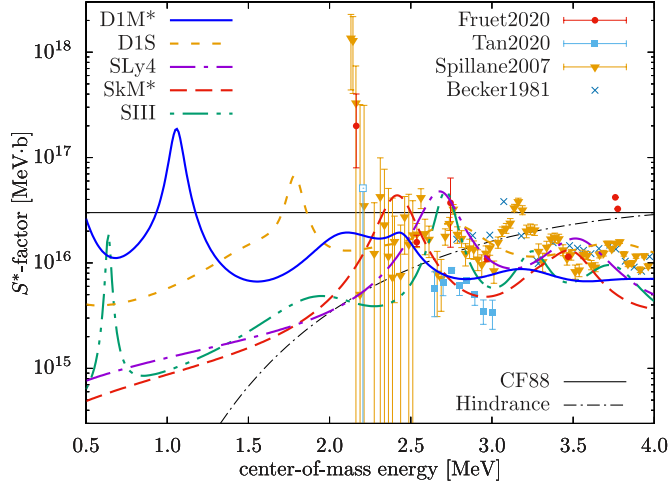


Figure 2:  $^{12}\text{C} + ^{12}\text{C}$  fusion  $S^*$ -factors obtained by using Skyrme and Gogny density functionals. The experimental data [40, 6, 8, 7], the evaluations by CF88 [10], and the hindrance model [11] are also shown.

where  $k$  is the wave number,  $F_l$  and  $G_l$  are the regular and irregular Coulomb functions, respectively, and  $\mu$  is the reduced mass.

To evaluate the  $S^*$ -factor, we calculate the  $^{12}\text{C} + ^{12}\text{C}$  fusion cross section, assuming that each resonance is narrow and isolated. In this case, the cross section at the center-of-mass energy  $E$  is given by the Breit-Wigner formula,

$$\sigma(E) = \frac{\pi \hbar^2 (2J+1)}{\mu E} \frac{\Gamma_0 \Gamma}{(E - E_R)^2 + \Gamma^2/4}, \quad (8)$$

where  $J$  and  $E_R$  denote the spin and energy of a resonance, respectively, and  $\Gamma_0$  is the partial width of the entrance channel ( $^{12}\text{C} + ^{12}\text{C}$ ). The total width  $\Gamma$  is estimated by a sum over the relevant channels,

$$\Gamma = \Gamma_{a_0} + \Gamma_{a_1} + \Gamma_{a_2} + \Gamma_{p_0} + \Gamma_{p_1} + \Gamma_{p_2}. \quad (9)$$

We note that this approximation may bring about additional uncertainty in the reaction rates. For instance, as seen in the results of D1M\* listed in Table 1, the  $2^+$  resonances at 2.10 and 2.45 MeV are close in energy and overlapping. In such cases, the shape of the cross section can deviate from that given by Eq. (8) due to the interference of the resonances. In principle, such resonance interference should be properly considered, but due to limitations in the framework of this study, it is neglected.

Given the cross section, the  $S^*$ -factor is defined as,

$$S^*(E) = E\sigma(E)/G^*(E), \quad (10)$$

with the modified Gamow parameter  $G^* = \exp(2\pi\eta + 0.46 \text{ MeV}^{-1}E)$ , and the Sommerfeld parameter  $\eta = 36/137 \sqrt{\mu c^2/2E}$  [39].

Figure 2 shows the calculated  $S^*$ -factors from all density functionals in comparison with the observed data and extrapolations. The resonance contributions appear as peak structures in the  $S^*$ -factor. In the  $E > 2.5$  MeV region, all density

functionals yield the  $S^*$ -factors with the same order of magnitude, which are roughly consistent with the observed data, but slightly lower than the CF88. On the other hand, there is striking difference in the low-energy region with  $E \lesssim 2$  MeV. The  $S^*$ -factors obtained from the Gogny D1M\* and D1S functionals yield prominent peaks at 1 and 1.8 MeV, which enhance the  $S^*$ -factor comparable with CF88. In contrast, the Skyrme functionals predict no significant peaks in this region, and their  $S^*$ -factors are closer to the hindrance model.

This remarkable difference in the  $S^*$ -factors originates in the low-energy  $0^+$  and  $2^+$  resonances, which are listed in Table 1 for the D1M\* and SkM\* functionals. For example, a notable peak at 1 MeV in the  $S^*$ -factor obtained by the D1M\* is created by the  $0^+$  and  $2^+$  resonances at 0.93 and 1.06 MeV, whereas they do not exist in the SkM\* results. We remark that the contributions from the  $2^+$  resonances are important. Since the peak height of the  $S^*$ -factor created by a single resonance is proportional to

$$(2J+1) \frac{P_C^{(l)}(a) \theta_C^2(a)}{G^*(E_R) \Gamma}, \quad (11)$$

the  $2^+$  resonance contributions are amplified by a factor of  $2J+1$  if other factors are the same order of magnitude. This is case for the  $2^+$  resonance at 1.06 MeV, and it manifests itself as a prominent peak at 1 MeV.

Thus, the deep sub-barrier resonances with  $J^\pi = 0^+$  and  $2^+$  potentially have large impact on the reaction rate, and hence, it is of utmost importance to experimentally search for them. We have suggested identifying the  $0^+$  resonances using their strong isoscalar monopole transitions as a probe [13]. This approach was successfully applied in an  $\alpha$ -inelastic scattering experiment [41], leading to the discovery of a  $0^+$  resonance at 1.38 MeV. Interestingly, this resonance is located between the  $0^+$  resonances obtained from the D1M\* and D1S functionals, which are located at 0.93 and 1.64 MeV, respectively. Therefore, the reality may lie somewhere between the predictions of D1M\* and D1S. Similarly, we suggest exploring the  $2^+$  resonances, which potentially have greater impact on the reaction rate, by means of the isoscalar quadrupole transitions. As shown in Table 1, the transition strengths of the  $2^+$  resonances are greater than the Weisskopf unit, thereby demonstrating the feasibility of this approach.

We also comment on the partial decay widths of the  $\alpha_0$  and  $p_0$  channels. In the recent particle- $\gamma$  coincidence measurements [6, 8, 7], these widths could not be measured. Therefore, they were estimated by assuming a linear dependence of the branching ratio on the energy [40]. Since we do not find such clear linearity in our results, it would be desirable to directly measure them. The  $\alpha$ -inelastic scattering experiments mentioned above, in principle, can measure the partial widths.

Finally, we discuss the nuclear reaction rate  $N_A \langle \sigma v \rangle$  which is defined as a function of temperature  $T$ ,

$$N_A \langle \sigma v \rangle = \sqrt{\frac{8}{\pi \mu}} \frac{N_A}{(k_B T)^{3/2}} \int_0^\infty E \sigma(E) e^{-\frac{E}{k_B T}} dE, \quad (12)$$

where  $N_A$  and  $k_B$  denote the Avogadro and Boltzmann constants, respectively. Figure 3 shows the  $^{12}\text{C} + ^{12}\text{C}$  fusion re-

Table 1: The properties of the  $J^\pi = 0^+$  and  $2^+$  resonances obtained by using the DIM\* and SkM\* density functionals. Only the resonances with energies ( $E_R$ ) lower than 4 MeV are listed.  $\Gamma$  is a total decay width, and  $\theta_C^2$  is a dimensionless reduced width amplitude for the  $^{12}\text{C} + ^{12}\text{C}$  channel in percent at channel radius  $a = 6$  fm (asterisked numbers are for  $a = 7$  fm). Branching ratios larger than  $10^{-2}$  are also listed.  $M(\text{IS}\lambda \uparrow)$  is the matrix element of the isoscalar monopole (quadrupole) transitions from the ground state of  $^{24}\text{Mg}$  to the  $J^\pi = 0^+$  ( $2^+$ ) resonances.

DF	$J^\pi$	$E_R$ [MeV]	$\Gamma$ [MeV]	$\theta_C^2$ [%]	branching ratio						$M(\text{IS}\lambda \uparrow)$ [W.u.]
					$\alpha_0$	$\alpha_1$	$\alpha_2$	$p_0$	$p_1$	$p_2$	
DIM*	$2^+$	0.40	0.14	0.6*	.31	.24		.19	.25		1.37
	$0^+$	0.93	0.47	4.8	.93	.04		.01			0.39
	$2^+$	1.06	0.10	1.1*	.54	.03		.27	.14		2.34
	$2^+$	2.10	0.45	0.6*	.40	.40		.02	.15		3.89
	$0^+$	2.33	0.63	8.8	.58	.38			.03		0.74
	$2^+$	2.45	0.18	0.2*	.08	.67		.09	.13		0.96
	$2^+$	3.21	0.67	5.8	.42	.46	.01	.03	.06	.01	3.68
	$0^+$	3.84	0.73	8.4	.26	.65	.02	.01	.04		1.07
	$2^+$	4.29	0.79	7.8	.30	.31	.16	.12	.07	.01	1.90
SkM*	$2^+$	2.42	0.36	1.2*	.01	.13		.53	.27	.05	3.23
	$2^+$	3.30	0.38	1.8	.20	.20		.20	.36	.01	1.42
	$0^+$	3.49	0.32	11.1	.65			.06	.27		0.94
	$2^+$	4.27	2.41	0.5*				.68	.26	.04	1.83

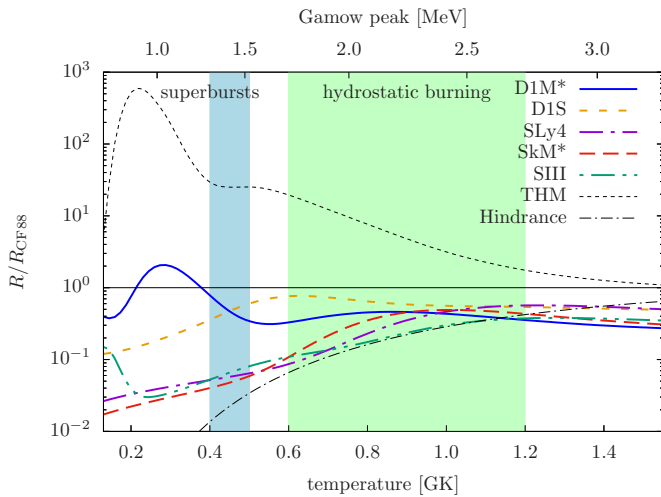


Figure 3: The  $^{12}\text{C} + ^{12}\text{C}$  fusion reaction rates relative to CF88 obtained by using the Gogny and Skyrme functionals. The upper scale shows the Gamow peak energies in MeV. The reaction rates obtained from the THM experiment [9] and the hindrance model [11] are also shown.

action rates relative to CF88, which exhibits the same trend as in the  $S^*$ -factor. At higher temperatures, all density functionals consistently yield the reaction rate slightly smaller than CF88. In contrast, at lower temperature  $T < 1$  GK, the Gogny and Skyrme functionals predict different behavior. The former give the reaction rates slightly smaller than CF88, whereas the latter give much hindered rates comparable with the hindrance model. We consider that the region enclosed by the reaction rates from the Gogny and Skyrme functionals is a constraint on the reaction rates imposed by the nuclear density functionals. The THM reaction rate is significantly higher than this, whereas the hindrance model approximates its lower limit. We also remark that, very recently, Dohi et al. [42] performed simulations of XRSB using these reaction rates (THM, CF88 and D1S) and found differences in the results that are sufficient to distinguish the THM rate from the others.

#### 4. Summary

Using a full-microscopic nuclear model with various nuclear density functionals, we have assessed the fusion reaction rate of  $^{12}\text{C} + ^{12}\text{C}$  at stellar temperatures. The reaction rates obtained from Gogny functionals are close to the CF88 estimation. In contrast, Skyrme functionals predict lower reaction rates, similar to the hindrance model. We interpret the intermediate region between the reaction rate obtained from the Gogny and Skyrme functionals as the constraints imposed by the nuclear density functionals.

The difference between the Gogny and Skyrme functionals owes to the  $J^\pi = 0^+$  and  $2^+$  resonances at deep sub-barrier energies. In the case of the Gogny functionals,  $^{12}\text{C} + ^{12}\text{C}$  molecular resonances appear approximately 1 MeV due to its coupling with other channels, leading to a substantial enhancement of the

reaction rate. On the other hand, in the case of the Skyrme functionals, such resonances appear slightly higher energies, and do not contribute to the reaction rate at low temperatures.

Hence, exploring the  $J^\pi = 0^+$  and  $2^+$  resonances at deep sub-barrier energy is a crucial step toward reducing the uncertainties in the reaction rate. For this purpose, we propose the measurements of the isoscalar transitions associated with these resonances. In particular, the  $2^+$  resonances, which potentially have great impact on the reaction rate, can be identified from their enhanced isoscalar dipole transitions.

We thank Dr. Nishimura and Dr. Dohi for helpful discussions. This work was partly supported by the RCNP Collaboration Research Network program as the project number COREnet-039. This research used computational resources of Wisteria/BDEC-01 Odyssey (the University of Tokyo), provided by the Multidisciplinary Cooperative Research Program in the Center for Computational Sciences, University of Tsukuba. This work was financially supported by the JSPS KAKENHI Grant Nos. 22K03610 and 22H01214.

## References

- [1] A. Cumming, L. Bildsten, Carbon flashes in the heavy-element ocean on accreting neutron stars, *The Astrophysical Journal* 559 (2001) L127–L130. doi:10.1086/323937.
- [2] T. E. Strohmayer, E. F. Brown, A remarkable 3 hour thermonuclear burst from 4u 1824-30, *The Astrophysical Journal* 566 (2002) 1045–1059. doi:10.1086/338337. URL <https://iopscience.iop.org/article/10.1086/338337>
- [3] W. D. Arnett, A possible model of supernovae: Detonation of  $^{12}\text{C}$ , *Astrophysics and Space Science* 5 (1969) 180–212. doi:10.1007/BF00650291/METRICS. URL <https://link.springer.com/article/10.1007/BF00650291>
- [4] K. Mori, M. A. Famiano, T. Kajino, M. Kusakabe, X. Tang, Impacts of the new carbon fusion cross-sections on type Ia supernovae, *Monthly Notices of the Royal Astronomical Society: Letters* 482 (2019) L70–L74. doi:10.1093/mnrasl/sly188. URL <https://academic.oup.com/mnrasl/article/482/1/L70/5115568>
- [5] S. E. Woosley, A. Heger, T. A. Weaver, The evolution and explosion of massive stars, *Rev. Mod. Phys.* 74 (2002) 1015–1071. doi:10.1103/RevModPhys.74.1015.
- [6] T. Spillane, F. Raiola, C. Rolfs, D. Schürmann, F. Strieder, S. Zeng, H.-W. Becker, C. Bordeanu, L. Gialanella, M. Romano, J. Schweitzer,  $\text{C}^{12}+\text{C}^{12}$  fusion reactions near the gamow energy, *Physical Review Letters* 98 (2007) 122501. doi:10.1103/PhysRevLett.98.122501. URL <https://link.aps.org/doi/10.1103/PhysRevLett.98.122501>
- [7] G. Fruet, S. Courtin, M. Heine, D. Jenkins, P. Adsley, A. Brown, R. Canavan, W. Catford, E. Charon, D. Curien, S. D. Negra, J. Duprat, F. Hammache, J. Lesrel, G. Lotay, A. Meyer, D. Montanari, L. Morris, M. Moukaddam, J. Nippert, Z. Podolyák, P. Regan, I. Ribaud, M. Richer, M. Rudigier, R. Shearman, N. de Séréville, C. Stodel, Advances in the direct study of carbon burning in massive stars, *Physical Review Letters* 124 (2020) 192701. doi:10.1103/PhysRevLett.124.192701. URL <https://link.aps.org/doi/10.1103/PhysRevLett.124.192701>
- [8] W. P. Tan, A. Boeltzig, C. Dulal, R. J. DeBoer, B. Frenzt, S. Henderson, K. B. Howard, R. Kelmar, J. J. Kolata, J. Long, K. T. Macon, S. Moylan, G. F. Peaslee, M. Renaud, C. Seymour, G. Seymour, B. V. Kolk, M. Wiescher, E. F. Aguilera, P. Amador-Valenzuela, D. Lizcano, E. Martínez-Quiroz, New measurement of  $\text{C}^{12}+\text{C}^{12}$ , *Physical Review Letters* 124 (2020) 192702. doi:10.1103/PhysRevLett.124.192702. URL <https://link.aps.org/doi/10.1103/PhysRevLett.124.192702>
- [9] A. Tumino, C. Spitaleri, M. L. Cognata, S. Cherubini, G. L. Guardo, M. Gulino, S. Hayakawa, I. Indelicato, L. Lamia, H. Petruscu, R. G. Pizzone, S. M. R. Puglia, G. G. Rapisarda, S. Romano, M. L. Sergi, R. Spartá, L. Trache, An increase in the  $^{12}\text{C} + ^{12}\text{C}$  fusion rate from resonances at astrophysical energies, *Nature* 557 (2018) 687–690. doi:10.1038/s41586-018-0149-4. URL <http://www.nature.com/articles/s41586-018-0149-4>
- [10] G. R. Caughlan, W. A. Fowler, Thermonuclear reaction rates v, *Atomic Data and Nuclear Data Tables* 40 (1988) 283–334. doi:10.1016/0092-640X(88)90009-5. URL <https://linkinghub.elsevier.com/retrieve/pii/0092640X8890009>
- [11] C. L. Jiang, K. E. Rehm, B. B. Back, R. V. F. Janssens, Expectations for  $\text{C}^{12}$  and  $\text{O}$ , *Physical Review C* 75 (2007) 015803. doi:10.1103/PhysRevC.75.015803. URL <https://link.aps.org/doi/10.1103/PhysRevC.75.015803>
- [12] R. L. Cooper, A. W. Steiner, E. F. Brown, Possible resonances in the  $^{12}\text{C} + ^{12}\text{C}$  fusion rate and superburst ignition, *The Astrophysical Journal* 702 (2009) 660–671. doi:10.1088/0004-637X/702/1/660. URL <https://iopscience.iop.org/article/10.1088/0004-637X/702/1/660>
- [13] Y. Taniguchi, M. Kimura,  $\text{C}^{12}+\text{C}^{12}$  fusion  $s$ -factor from a full-microscopic nuclear physics, *Physics Letters B* 823 (2021) 136790. doi:10.1016/j.physletb.2021.136790. URL <https://linkinghub.elsevier.com/retrieve/pii/S03702693210073>
- [14] D. L. Hill, J. A. Wheeler, Nuclear constitution and the interpretation of fission phenomena, *Physical Review* 89 (1953) 1102–1145. doi:10.1103/PhysRev.89.1102.
- [15] J. J. Griffin, J. A. Wheeler, Collective motions in nuclei by the method of generator coordinates, *Physical Review* 108 (1957) 311–327. doi:10.1103/PhysRev.108.311.
- [16] J. F. Berger, M. Girod, D. Gogny, Time-dependent quantum collective dynamics applied to nuclear fission, *Computer Physics Communications* 63 (1991) 365–374. doi:10.1016/0010-4655(91)90263-K.
- [17] C. Gonzalez-Boquera, M. Centelles, X. Viñas, L. Robledo, New gogny interaction suitable for astrophysical applications, *Physics Letters B* 779 (2018) 195–200. doi:10.1016/j.physletb.2018.02.005. URL <https://linkinghub.elsevier.com/retrieve/pii/S03702693183010>
- [18] P. Bauer, P. Quentin, M. Brack, C. Guet, B. Häkansson, Towards a better parametrisation of skyrme-like effective forces: A critical study of  $\text{N}^{14}$ , *Nuclear Physics A* 386 (1982) 79–100. doi:10.1016/0375-9474(82)90403-1. URL <https://linkinghub.elsevier.com/retrieve/pii/037594748290403>
- [19] E. Chabanat, P. Bonche, P. Haensel, J. Meyer, R. Schaeffer, A skyrme parametrization from subnuclear to neutron star densities part ii. nuclei far from stability, *Nuclear Physics A* 635 (1998) 231–256. doi:10.1016/S0375-9474(98)00180-8. URL <https://linkinghub.elsevier.com/retrieve/pii/S03759474980018>
- [20] E. Chabanat, P. Bonche, P. Haensel, J. Meyer, R. Schaeffer, Erratum: A skyrme parametrization from subnuclear to neutron star densities part ii.  $\text{N}^{14}$ , *Nuclear Physics A* 643 (1998) 441. doi:10.1016/S0375-9474(98)00570-3. URL <https://linkinghub.elsevier.com/retrieve/pii/S03759474980057>
- [21] M. Beiner, H. Flocard, N. V. Giai, P. Quentin, Nuclear ground-state properties and self-consistent calculations with the skyrme interaction, *Nuclear Physics A* 238 (1975) 29–69. doi:10.1016/0375-9474(75)90338-3. URL <https://linkinghub.elsevier.com/retrieve/pii/037594747590338>
- [22] Y. Kanada-En’yo, M. Kimura, A. Ono, Antisymmetrized molecular dynamics and its applications to cluster phenomena, *Progress of Theoretical and Experimental Physics* 2012 (2012) 01A202.
- [23] Y. Taniguchi, M. Kimura, H. Horiuchi, New constraint of clustering for  $\text{C}^{12}$  and its application to the study of the  $^{2-12}\text{C}$  structure, *Progress of Theoretical Physics* 112 (2004) 475–487. doi:10.1143/PTP.112.475. URL <https://academic.oup.com/ptp/article-lookup/doi/10.1143/PTP.112.475>
- [24] A. Doté, H. Horiuchi, Y. Kanada-En’yo, Antisymmetrized molecular dynamics plus hartree-fock model and its application to be isotopes, *Phys. Rev. C* 56 (1997) 1844–1854. doi:10.1103/PhysRevC.56.1844.
- [25] E. Almqvist, D. A. Bromley, J. A. Kuehner, Resonances in  $\text{C}^{12}$  on carbon reactions, *Physical Review Letters* 4 (1960) 515–517. doi:10.1103/PhysRevLett.4.515. URL <https://link.aps.org/doi/10.1103/PhysRevLett.4.515>
- [26] E. Almqvist, D. A. Bromley, J. A. Kuehner, B. Whalen, Spins and partial widths of quasimolecular resonances in  $\text{C}^{12} + \text{C}^{12}$  interactions,

- Physical Review 130 (1963) 1140–1152.  
doi:10.1103/PhysRev.130.1140.  
URL <https://link.aps.org/doi/10.1103/PhysRev.130.1140>
- [27] M. G. Mazarakis, W. E. Stephens, Experimental measurements of the  $c12 + c12$  nuclear reactions at low energies, Physical Review C 7 (1973) 1280–1287.  
doi:10.1103/PhysRevC.7.1280.  
URL <https://link.aps.org/doi/10.1103/PhysRevC.7.1280>
- [28] E. R. Cosman, T. M. Cormier, K. V. Bibber, A. Spurduto, G. Young, J. Erskine, L. R. Greenwood, O. Hansen, Evidence for a  $c12 + c12$  collective band in  $mg24$ , Physical Review Letters 35 (1975) 265–268. doi:10.1103/PHYSREVLETT.35.265.  
URL <https://journals.aps.org/prl/abstract/10.1103/PhysRevLett.35.265>
- [29] Z. Basrak, F. Auger, B. Fernandez, J. Castebois, N. Cindro, Spins of resonances in the  $12c + 12c$  system, Physics Letters B 65 (1976) 119–121. doi:10.1016/0370-2693(76)90008-3.  
URL <https://linkinghub.elsevier.com/retrieve/pii/0370269376900083>
- [30] K. A. Erb, R. R. Betts, D. L. Hanson, M. W. Sachs, R. L. White, P. P. Tung, D. A. Bromley, New resonances in the low-energy  $c12 - c12$  spectrum, Physical Review Letters 37 (1976) 670–673. doi:10.1103/PhysRevLett.37.670.  
URL <https://link.aps.org/doi/10.1103/PhysRevLett.37.670>
- [31] N. R. Fletcher, J. D. Fox, G. J. KeKelis, G. R. Morgan, G. A. Norton, Resonant structures in the  $c12(c12, be8)o16$  reaction,  $ec.m.=9$  to 20 mev, Physical Review C 13 (1976) 1173–1179.  
doi:10.1103/PHYSREVC.13.1173.  
URL <https://journals.aps.org/prc/abstract/10.1103/PhysRevC.13.1173>
- [32] R. Wada, J. Shimizu, K. Takimoto, Sub-coulomb resonances in the  $c12-c12$  system through the reaction  $c12(c12, o16)be8$ , Physical Review Letters 38 (1977) 1341–1344.  
doi:10.1103/PHYSREVLETT.38.1341.  
URL <https://journals.aps.org/prl/abstract/10.1103/PhysRevLett.38.1341>
- [33] H. T. Fortune, L. R. Greenwood, R. E. Segel, J. R. Erskine, Resonances in  $c12(c12, a)ne20$ , Physical Review C 15 (1977) 439–443. doi:10.1103/PHYSREVC.15.439.  
URL <https://journals.aps.org/prc/abstract/10.1103/PhysRevC.15.439>
- [34] M. Ohkubo, K. Kato, H. Tanaka,  $12c + 12c$  molecule-like structure in  $24mg$ : A study of the  $12c + 12c$  system by the coupled channel orthogonality condition model, Progress of Theoretical Physics 67 (1982) 207–221.  
doi:10.1143/PTP.67.207.  
URL <https://academic.oup.com/ptp/article-lookup/doi/10.1143/PTP.67.207>
- [35] A. M. Lane, R. G. Thomas, R-matrix theory of nuclear reactions, Reviews of Modern Physics 30 (1958) 257–353.  
doi:10.1103/RevModPhys.30.257.  
URL <https://link.aps.org/doi/10.1103/RevModPhys.30.257>
- [36] G. Breit, E. Wigner, Capture of slow neutrons, Physical Review 49 (1936) 519–531. doi:10.1103/PhysRev.49.519.  
URL <https://link.aps.org/doi/10.1103/PhysRev.49.519>
- [37] Y. Kanada-En'yo, T. Suhara, Y. Taniguchi, Approximation of reduced width amplitude and application to cluster decay width, Progress of Theoretical and Experimental Physics 2014 (2014) 073D02.  
doi:10.1093/ptep/ptu095.  
URL <https://academic.oup.com/ptep/article-lookup/doi/10.1093/ptep/ptu095>
- [38] Y. Chiba, M. Kimura, Laplace expansion method for the calculation of the reduced-width amplitudes, Progress of Theoretical and Experimental Physics 2017 (2017) 053D01.
- [39] J. R. Patterson, H. Winkler, C. S. Zaidins, Experimental investigation of the stellar nuclear reaction  $12c + 12c$  at low energies, The Astrophysical Journal 157 (1969) 367. doi:10.1086/150073.  
URL <http://adsabs.harvard.edu/doi/10.1086/150073>
- [40] H. W. Becker, K. U. Kettner, C. Rolfs, H. P. Trautvetter, The  $12c+12c$  reaction at subcoulomb energies (ii), Zeitschrift für Physik A Atoms and Nuclei 303 (1981) 305–312.  
doi:10.1007/BF01421528.  
URL <https://link.springer.com/article/10.1007/BF01421528>  
<http://link.springer.com/10.1007/BF01421528>
- [41] P. Adsley, M. Heine, D. Jenkins, S. Courtin, R. Neveling, J. Brümmer, L. Donaldson, N. Kheswa, K. Li, D. Marín-Lámbarri, P. Mabika, P. Papka, L. Pellegrini, V. Pesudo, B. Rebeiro, F. Smit, W. Yahia-Cherif, Extending the hoyle-state paradigm to  $c12+c12$  fusion, Physical Review Letters 129 (2022) 102701.  
doi:10.1103/PhysRevLett.129.102701.  
URL <https://link.aps.org/doi/10.1103/PhysRevLett.129.102701>
- [42] A. Dohi, N. Nishimura, H. Sotani, T. Noda, H.-L. Liu, S. Nagataki, M. Hashimoto, Impacts of the direct urca and superfluidity inside a neutron star on type i x-ray burst, The Astrophysical Journal 937 (2022) 124.  
doi:10.3847/1538-4357/ac8dfe.  
URL <https://iopscience.iop.org/article/10.3847/1538-4357/ac8dfe>